Fabrication of Nanoporous Gold Film Electrodes with Ultrahigh Surface Area and Electrochemical Activity

Falong Jia, Chuanfang Yu, Zhihui Ai, and Lizhi Zhang*

Key Laboratory of Pesticide & Chemical Biology of Ministry of Education, College of Chemistry, Central China Normal University, Wuhan 430079, P. R. China

Received February 13, 2007. Revised Manuscript Received May 28, 2007

Nanoporous gold film (NPGF) electrode was fabricated by applying multicyclic potential scans on a polished gold electrode in an electrolyte composed of $ZnCl_2$ and benzyl alcohol. In the cathodic potential scan, Zn was first electrodeposited on the gold electrode surface, and Au−Zn alloy was then directly formed on the surface under an elevated temperature. In the subsequent anodic potential scan, dealloying of Zn took place, resulting in a nanostructured gold film. Furthermore, Zn was then electrodeposited onto the porous gold surface and a Au−Zn alloy was formed at the same time. Through controlling the parameters of cyclic voltammetry and cyclic times, we finally obtained a three-dimensional NPGF with nanopores. The resulting NPGF possessed ultrahigh roughness factor and surface area. Results showed that the electrochemical activity of the NPGF electrode was much higher than that of the polished gold electrode. We believe that the resulting NPGF electrode is promising in the fields of catalysis, sensors, and so on. Meanwhile, this multicyclic electrochemical alloying/dealloying method may be applied to fabricate other nanoporous metal films.

1. Introduction

High-surface-area nanoporous gold had attracted great interest for their wide applications as catalysts, sensors, and actuators.[1−3] Compared with the gold-nanoparticle-modified electrode obtained using the adsorbing method, the gold electrode with nanoporous structure possessed a much higher surface area and better electron transport, which led to distinguished performance in trace ion analysis.[4] In addition, the porous structure of the gold electrode offered a great number of adsorption sites for proteins and enzymes, which would make nanoporous gold attractive in biosensors. It was reported that nanoporous gold could be prepared by electrochemical deposition,[5] a liquid-crystal template technique,[6] organic templating,[7−9] "direct freezing",[10] and a voltage-induced dimension change method.[11]

Dealloying is a kind of corrosion process to separate components of alloy by selective dissolution. For instance, if component B is more reactive than A in binary alloy A_xB_{1-x}, B will be dissolved from the alloy while A will remain during a dealloying process. Previous studies on selective dissolution mainly focused on corrosion.[12−14] In recent years, the dealloying process was found to be an effective route to fabricating nanoporous gold. For instance, Erlebacher and his co-workers researched the evolution of porosity in the dealloying process of Au−Ag alloy.[15] They proposed a numerical model to simulate the alloy dissolution and demonstrated that the formation of nanopores in gold was attributed to an intrinsic dynamic pattern formation process.[15] Besides chemical etching of Ag from Au−Ag alloy,[16] electrochemical dealloying was also performed to obtain nanoporous Au films with high mechanic integrity.[17]

In most works, Au−Ag alloy was normally used as a starting material to fabricate nanoporous gold. The Au−Ag alloy was prepared by metal melting. The thickness of the Au−Ag alloy was then thinned by "beating" or cold-rolling.[16] In that case, the dealloyed Au film was only 100 nm in thickness, so its low mechanic strength may make it undesirable as an independent electrode. Meanwhile, complete dealloying of Ag from Au−Ag alloy was necessary in order to avoid the electrochemical signals from Ag for the subsequent electroanalytical application. This increased the difficulty in fabricating nanoporous gold film with desirable thickness if Au−Ag alloy was utilized. Recently, Sun and his co-workers reported an interesting method to fabricate

* To whom correspondence should be addressed. E-mail: zhanglz@mail.ccnu.edu.cn. Tel/Fax: 86-27-6786 7535.

(1) Ding, Y.; Chen, M. W.; Erlebacher, J. *J. Am. Chem. Soc.* **2004**, *126*, 6876.
(2) Bonroy, K.; Friedt, J.-M.; Frederix, F.; Laureyn, W.; Langerock, S.; Campitelli, A.; Sara, M.; Borghs, G.; Goddeeris, B.; Declerck, P. *Anal. Chem.* **2004**, *76*, 4299.
(3) Kramer, D.; Viswanath, R. N.; Weissmüller, J. *Nano Lett.* **2004**, *4*, 793.
(4) Huang, J. F.; Sun, I. W. *Adv. Funct. Mater.* **2005**, *15*, 989.
(5) Shin, H. C.; Dong, J.; Liu, M. L. *Adv. Mater.* **2003**, *15*, 1610.
(6) Luo, H.; Sun, L.; Lu, Y.; Yan, Y. S. *Langmuir* **2004**, *20*, 10218.
(7) Zhang, H.; Hussain, I.; Brust, M.; Cooper, A. I. *Adv. Mater.* **2004**, *16*, 27.
(8) Walsh, D.; Arcelli, L.; Ikoma, T.; Mann, J. T. *Nat. Mater.* **2003**, *2*, 386.
(9) Shchukin, D. G.; Caruso, R. A. *Chem. Commun.* **2003**, 1478.
(10) Zhang, H.; Hussain, I.; Brust, M.; Butler, M. F.; Rannard, S. P.; Cooper, A. I. *Nat. Mater.* **2005**, *4*, 787.
(11) Weissmüller, J.; Viswanath, R. N.; Kramer, D.; Zimmer, P.; Würschum, R.; Gleiter, H. *Science* **2003**, *300*, 312.
(12) Pickering, H. W. *Corros. Sci.* **1983**, *23*, 1107.
(13) Williams, D. E.; Newman, R. C.; Song, Q.; Kelly, R. G. *Nature* **1991**, *350*, 216.
(14) Newman, R. C.; Sieradzki, K. *Science* **1994**, *263*, 1708.
(15) Erlebacher, J.; AzizM, J.; Karma, A.; Dimitrov, N.; Sieradzki, K. *Nature* **2001**, *410*, 450.
(16) Ding, Y.; Kim, Y. J.; Erlebacher, J. *Adv. Mater.* **2004**, *16*, 1897.
(17) Senior, N. A.; Newman, R. C. *Nanotechnology* **2006**, *17*, 2311.

10.1021/cm070425l CCC: $37.00
Published on Web 06/30/2007

Scheme 1. Schematic Illustration of the Formation of NPGF Electrode by a Multicyclic Electrochemical Alloying/Dealloying Method

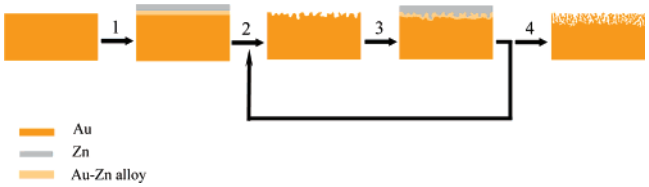

Step 1, electrodeposition of Zn and formation of Au−Zn alloy; step 2, electrochemical dealloying; step 3, electrodeposition of Zn and formation of Au−Zn alloy again; step 4, formation of NPGF after multicyclic alloying/dealloying.

NPGF directly on the surface of a gold electrode with a single-cycle electrochemical alloying/dealloying process in an ionic liquid containing $ZnCl_2$, by making use of a Au−Zn alloy.[4] However, their fabrication process must be conducted in a glove box free of oxygen and water because of the strict requirement of the ionic liquid. These special experimental requirements may hinder the large-scale application of this attractive method. Therefore, it is still a challenge to develop a convenient and green method to fabricate NPGF electrodes with high surface areas.

Here, for the first time, we report a one-pot green route for directly fabricating NPGF on gold electrodes through multicyclic electrochemical alloying/dealloying processes in a novel electrolyte composed of $ZnCl_2$ and benzyl alcohol (BA) (Scheme 1). In the cathodic potential scan, Zn was first electrodeposited on gold electrode surface, and Au−Zn alloy was then directly formed on the surface at an elevated temperature (step 1). In the subsequent anodic potential scan, dealloying of Zn took place (step 2), resulting in the formation of a nanostructured gold film. In step 3, Zn was then electrodeposited onto the porous gold surface and Au−Zn alloy was formed at the same time. Through controlling the parameters of cyclic voltammetry and cyclic times, a three-dimensional NPGF electrode with nanopores was finally produced (step 4). All these processes could be performed in one pot without any special protection. Compared with ionic liquids, benzyl alcohol is inexpensive, very stable, and not sensitive to oxygen. It has been utilized for the synthesis of different nanostructured oxides.[18−21] Moreover, the boiling point of benzyl alcohol is relatively high. This makes it possible for the direct formation of metal alloys in the electrolyte under elevated temperatures.

2. Experimental Section

Reagents and Instrumentation. Zinc chloride (99.9%), benzyl alcohol (99%), gold wire (99.99%, 0.2 mm in diameter), zinc plate (99.99%), and platinum plate (99.99%) were purchased from the Shanghai Chemical Company. All solutions were prepared using deionized water (>18 MΩ cm). All electrochemical experiments were performed on an electrochemical workstation (CHI660B, CHI Instruments, Shanghai). Field-emission scanning electron microscopy (FESEM) and energy-dispersive X-ray spectrometer (EDS) measurements were performed using JEOL-6700F and Oxford INCA.

Preparation of Nanoporous Gold Film Electrode. The fabrication process was carried out in the $ZnCl_2$/BA electrolyte in air. The electrolyte was prepared by dissolving anhydrous $ZnCl_2$ in BA at 60 °C, and the concentration of $ZnCl_2$ was 1.6 M. The electrolyte was not deaerated in the whole process of experiment and all the alloying/dealloying processes were performed under ambient atmosphere. Multicyclic electrochemical alloying/dealloying on gold electrode (gold wire) was realized in a three-electrode cell, which consisted of Zn plate as the auxiliary electrode, Zn wire as the reference electrode and gold wire as the working electrode, respectively. These three electrodes were placed in the same cell without a salt-bridge connection. The gold electrode was polished; cleaned by acetone, alcohol and deionized water; and dried before use. The geometric area of the gold electrode exposed to the electrolyte was 3.82 mm^2. The electrochemical window of benzyl alcohol was found to be in the potential range of 1.88 to −0.72 V (vs Zn). So we chose this potential range to perform the alloying/dealloying processes. A multicyclic potential sweep was applied to the working electrode at a scan rate of 10 mV s^{-1} on the electrochemical workstation. The first cycle should be in the sequence of open circuit → −0.72 → 1.88 V (vs Zn), and the later cycles were from 1.88 to −0.72 V (vs Zn) repeatedly. After a certain number of cycles, the gold electrode was taken out and cleaned quickly by benzyl alcohol, ethanol, and deionized water in sequence.

Electrochemical Measurements. All the electrochemical analyses were carried out at room temperature in a three-electrode cell, with Pt plate as the auxiliary electrode, saturated calomel electrode (SCE) as the reference electrode, and the NPGF electrode as the working electrode, respectively. Before each experiment, the NPGF electrode was cleaned in 0.5 M H_2SO_4 solution by cyclic scan from 0.4 to 1.5 V (vs SCE) until reproductive curves were obtained. The solution for dopamine analysis was freshly prepared by dissolving dopamine in 0.1 M pH 7.1 phosphate buffer solution, which had been deaerated by purging with high-purity nitrogen. The detection of dopamine was carried out at ambient temperature under a nitrogen atmosphere.

3. Results and Discussion

3.1. Effect of Temperature and Cyclic Times on the Alloying/Dealloying Process of Gold. Figure 1a shows the tenth cyclic voltammetry (CV) curves of a polished gold electrode in a $ZnCl_2$/BA electrolyte at different temperatures. The open circuit of the polished gold electrode in $ZnCl_2$/BA electrolyte was about 1.12 V. When the potential moved from the open circuit toward −0.72 V, the surface of the gold gradually became white, indicating the deposition of Zn on the surface. In the CV curve performed at 20 °C, there was only a single anodic peak at 0.85 V, which resulted from the oxidation of Zn. After ten cycles, the morphology of the gold electrode did not change much according to the scanning electron microscopy observation. This indicated that alloying/dealloying process did not happen at this room temperature. When the temperature increased to 80 °C, the current value increased a lot. From 100 to 120 °C, another anodic peak (1.35−1.44 V) appeared. This peak was attributed to the oxidation of the Au−Zn alloy. With the increase in temperature, it was found that the current increment of the second anodic peak (1.35−1.45 V) was much higher than that of

(18) Niederberger, M.; Garnweitner, G.; Pinna, N.; Neri, G. *Prog. Solid State Chem.* **2005**, *33*, 59.
(19) Niederberger, M.; Garnweitner, G. *Chem.—Eur. J.* **2006**, *12*, 7282.
(20) Niederberger, M.; Pinna, N.; Polleux, J.; Antonietti, M. *Angew. Chem., Int. Ed.* **2004**, *43*, 2270.
(21) Niederberger, M.; Garnweitner, G.; Pinna, N.; Antonietti, M. *J. Am. Chem. Soc.* **2004**, *126*, 9120.

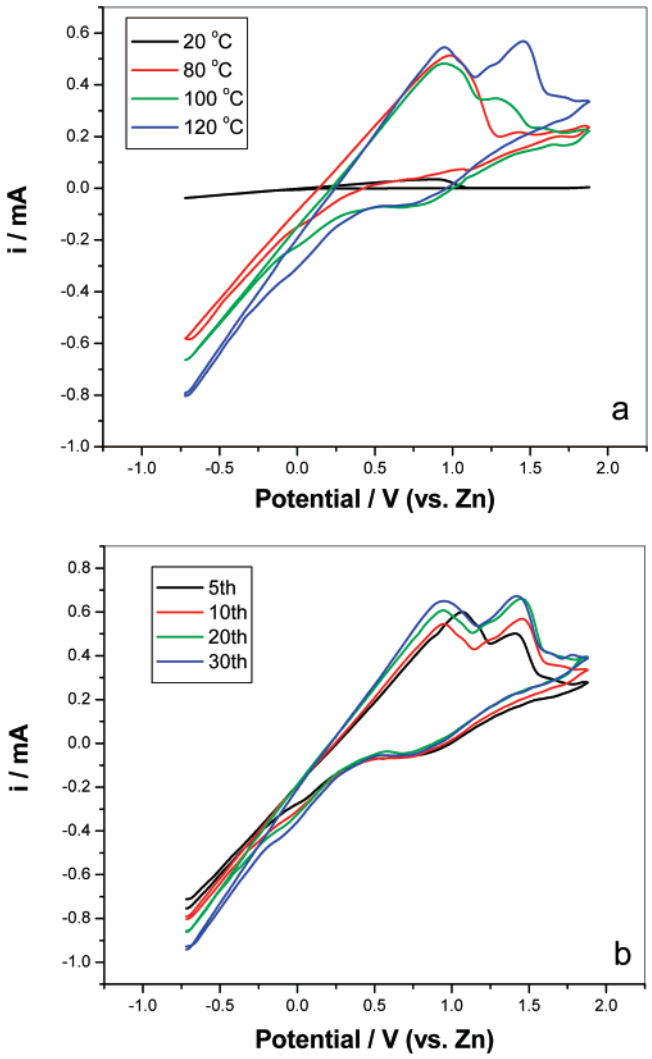

Figure 1. (a) Tenth cyclic voltammetry curves of a polished gold electrode in $ZnCl_2$/BA electrolyte at different temperatures of 20, 80, 100, and 120 °C. (b) Cyclic voltammetry curves of a polished gold electrode in $ZnCl_2$/BA electrolyte at 120 °C under different numbers of cycles: 5, 10, 20, and 30; scan rate = 10 mV s^{-1}.

the first anodic peak (0.84−1.03 V), indicating that more deposited Zn formed Au−Zn alloy at higher temperature. In Figure 1a, a reduction wave (1.0−0.5 V) was observed at temperature of 100 and 120 °C. However, this reduction wave was not observed at lower temperature or for the first cycle at 100 and 120 °C. Therefore, this wave probably resulted from the deposition of Zn on the porous gold formed after several cycles. Obviously, the porous surface decreased the nucleation potential and favored the deposition of Zn on the gold. After the porous gold was covered with a Zn layer, the subsequent deposition took place on the Zn. The second reduction wave at 0 V was very weak. It may be attributed to the reduction of the $Zn(BA)_x^{2+}$ complex. We found that the conductivity of the $ZnCl_2$/benzyl alcohol solution increased from 0.056 to 0.38 mS m^{-1} with the concentration of $ZnCl_2$ increasing from 0.01 to 0.1 M. The conductivity was improved with the increase of $ZnCl_2$ concentration, indicating the existence of zinc(II) in benzyl alcohol with an ionic nature, not neutral.

From the above results, we conclude that the Au−Zn alloy could be formed on the gold surface at temperatures higher than 100 °C. In the later experiments, the alloying/dealloying process of gold electrode was performed at 120 °C.

To determine the optimum cycle times of the alloying/dealloying process, we recorded CV curves with different cycle times (Figure 1b). When the duration time of the cycles increased, the current of anodic peak at 1.44 V first increased quickly (from the 5th to 20th cycle) and then changed little (from the 20th to 30th cycle). This phenomenon can be explained as follows. The gold surface became coarse at the beginning of the alloying/dealloying process, providing more sites for alloying with Zn. As a result, the current of oxidation peak of Au−Zn alloy increased a lot from the 5th to 20th cycle. However, the surface of coarse gold would remain almost unchanged when the number of cycles reached a certain value (after 20 cycles), because the deposition of Zn on the interior region of nanostructured gold became very difficult in view of the diffusion polarization of Zn^{2+} ions at that time. Therefore, the current of the oxidation peak of Au−Zn alloy could not increase any more.

Figure 2 shows the field-emission scanning electron microscopy (FESEM) images of gold electrodes after different cycle times of alloying/dealloying in $ZnCl_2$/BA electrolyte at 120 °C. We found that the morphology of the gold electrode was affected greatly by the total cycle times. After 10 cycles of alloying/dealloying, the gold surface turned brown-red and the porous structure could be easily observed on the SEM image (Figure 2a). However, the pore size was still very large and the porosity was low. Interestingly, the color of the gold surface became dark after 30 cycles. A well-defined three-dimensional nanoporous structure was formed (Figure 2b). The roughness was obviously much higher than that formed after 10 cycles. The ligament and pore size were about 60 and 100 nm, respectively. Obviously, the nanoporous gold film electrode obtained after 30 cycles had a higher surface area. We also tried more alloying/dealloying (40 cycles); the resulting gold film possessed a nanoporous structure similar to that of the 30-cycle NPGF. We repeated the experiments many times and found that the multicyclic electrochemical alloying/dealloying processes were well-reproduced.

Figure 3 displays the cross-sectional scanning electron microscopy images of gold electrodes prepared under the same conditions as those of panels a and b in Figure 2. The thickness of the porous film formed after 10 alloying/dealloying cycles was estimated to be about 1 μm, and the porosity of the electrode was low. After 30 cycles, the porosity improved a lot and the thickness of porous film was about 5 μm. The accessible range of nanopore sizes was from about 30 to 200 nm by adjusting the cyclic times. The distribution of the pore size within the film (along the depth of the film) was not very large. Near the substrate, a certain amount of big pores (like nanocaves) with sizes of ~200 nm coexisted with smaller pores with sizes of ~50 nm. These nanocaves could probably arise from the plastic deformation during the electrochemical dealloying.[22]

Less than 6 atom % Zn was found in the NPGF electrode on the basis of EDS analysis. A similar phenomenon was

(22) Parida, S.; Kramer, D.; Volkert, C. A.; Rösner, H.; Erlebacher, J.; Weissmüller, J. *Phys. Rev. Lett.* **2006**, *97*, 035504.

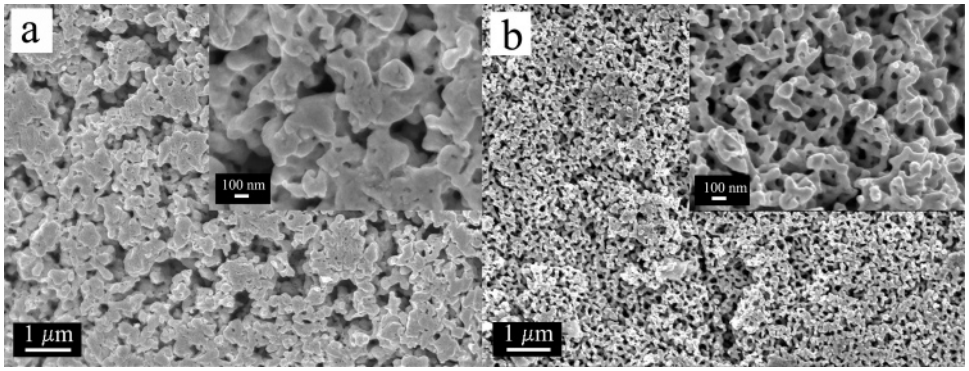

Figure 2. Field-emission scanning electron microscopy images of gold electrodes after different cycle times of alloying/dealloying in $ZnCl_2$/BA electrolyte at 120 °C. (a) 10 cycles; (b) 30 cycles.

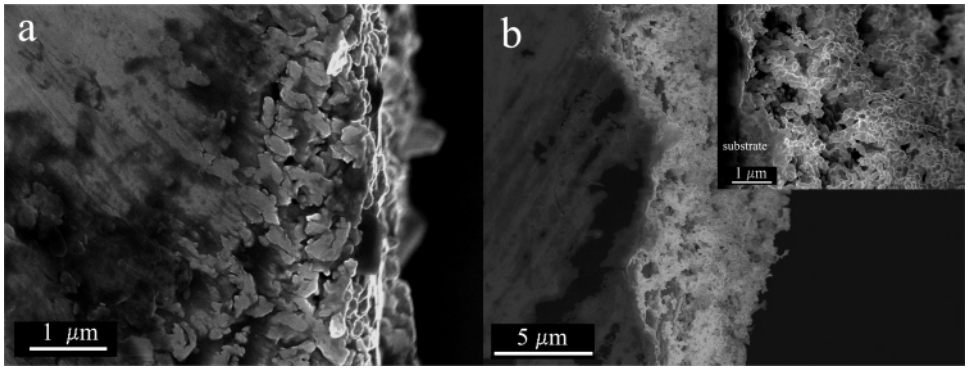

Figure 3. Cross-sectional view of gold electrodes after alloying/dealloying in $ZnCl_2$/BA electrolyte at 120 °C for (a) 10 and (b) 30 cycles. The inset in b is the corresponding image with higher magnification.

also observed for dealloying of Au−Ag alloy.[16,17,22] We thought such trace amounts of Zn did not affect the property of NPGF electrode much, because the NPGF electrode exhibited the same electrochemical behavior as that of pure gold.

3.2. Electrochemical Behavior of the Nanoporous Gold Film Electrode. It was known that the roughness factor was normally used to express the ratio between the real surface area and the geometrical area of electrode. In the case of the gold electrode, the charge associated with the reduction of gold oxide was proportional to the real active surface area of gold electrode.[23] In this work, CV in 0.5 M H_2SO_4 solution was employed to compare the electrochemically active surface area of gold electrodes before and after the alloying/dealloying process (Figure 4). In Figure 4, there was a symmetrical cathodic peak at 0.88 V, resulting from the electrochemical reduction of gold oxide that formed at the anodic scan. By integrating the charge consumed in the gold oxide reduction, we estimated the roughness factors of NPGF electrodes after 10 and 30 cycles to be about 55 and 560, respectively. The value of 560 was much higher than that (213.7) of nanoporous gold electrode obtained by the alloying/dealloying of gold electrodes in the ionic liquid (1-ethyl-3-methylimidazolium) containing $ZnCl_2$.[4] Therefore, we conclude that our multicyclic alloying/dealloying method in benzyl alcohol is very efficient for fabricating a three-dimensional nanoporous gold film with ultrahigh surface area.

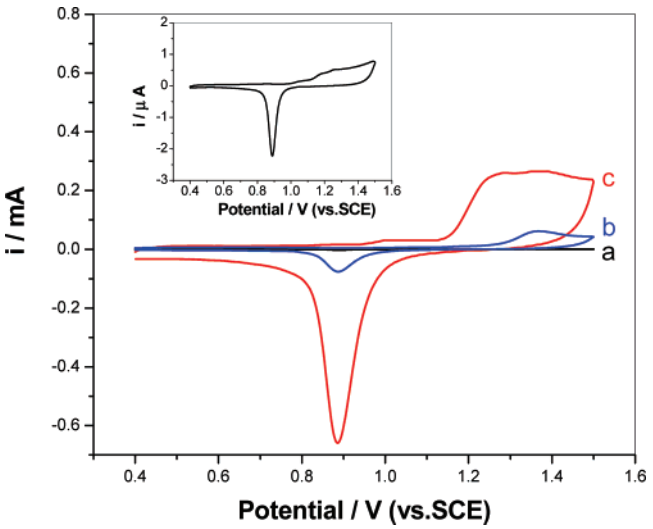

Figure 4. CV curves recorded in 0.5 M H_2SO_4 for the (a) polished gold electrode and (b, c) the nanoporous gold electrodes; scan rate = 100 mV s^{-1}. The inset is the magnified curve of a. The nanoporous gold electrodes were obtained after (b) 10 and (c) 30 alloying/dealloying cycles of the polished gold electrode at 120 °C.

Cyclic voltammetry of $Fe(CN)_6^{3-/4-}$ was a typical method to test the kinetics of electrode interface. For a nonporous gold electrode, the redox current value was proportional to its geometric area. Because the NPGF electrode had a larger active area than the polished gold, it would be expected that the redox current of $Fe(CN)_6^{3-/4-}$ was also much higher than that of the polished gold. We found that the redox current of $Fe(CN)_6^{3-/4-}$ at the NPGF electrode was about six times that at the polished one (Figure 5a). Meanwhile, the corresponding square wave voltammetry (SWV) results also

(23) Trasatti, S.; Petrii, O. A. *Pure Appl. Chem.* **1991**, *63*, 711.

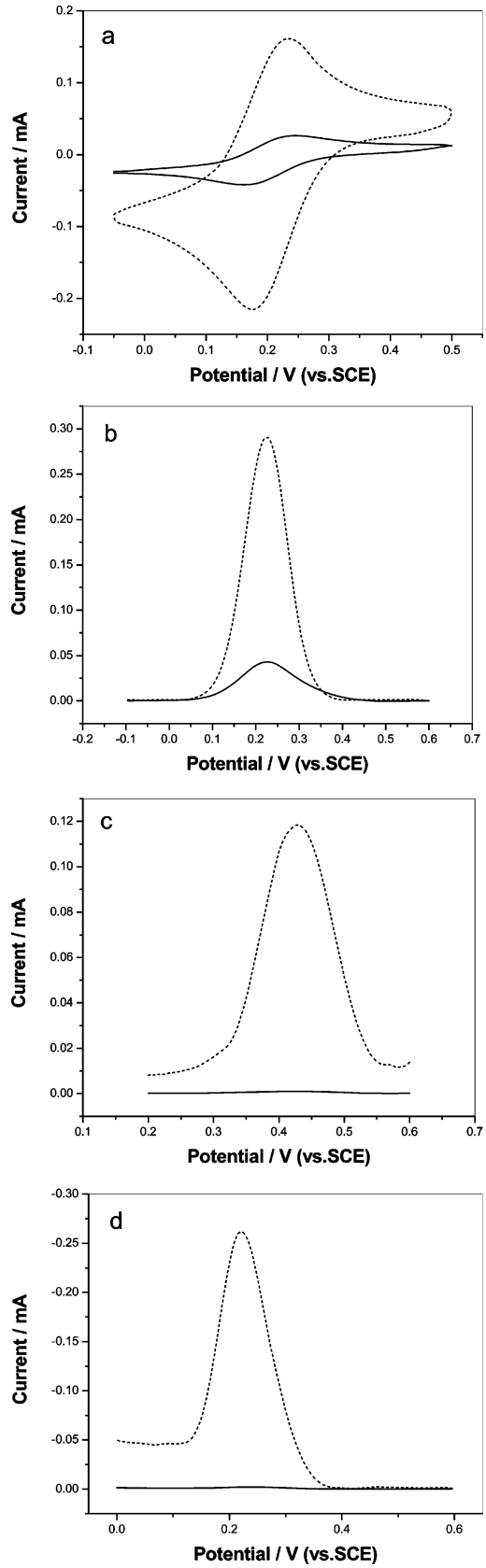

Figure 5. Comparison of electrochemical behavior of the NPGF electrode (dashed line) and the polished gold electrode (solid line) in different systems. (a) CV curves of 10 mM $Fe(CN)_6^{3-/4-}$ in 0.1 M KCl solution, scan rate = 50 mV s^{-1}; (b) square wave voltammetry curves of 10 mM $Fe(CN)_6^{3-/4-}$ in 0.1 M KCl solution; (c) square wave voltammetry curves of 10 mM NH_4FeSO_4 in 0.1 M KCl solution; (d) square wave voltammetry curves of 1 mM Cu^{2+} in 0.1 M phosphate buffer solution (pH 5.0). All these square wave voltammetry curves were obtained under a frequency of 50 Hz, increments of 4 mV, and amplitude of 25 mV.

showed that the anodic current at the NPGF electrode was about eight times that at the polished gold one (Figure 5b). Obviously, the increase in redox current of $Fe(CN)_6^{3-/4-}$ at the NPGF electrode was not as much as that of surface area. A similar phenomenon was observed by Kuhn and his coworkers.[24] They found that the electrochemical signal at the macroporous gold electrode was about one and half times that of a flat one, although the surface area of the macroporous gold electrode was about 10 times higher.[24] According to Kuhn's viewpoint, this phenomenon could be explained by the fast kinetics of the redox couple at the outermost layer. In this case, the inner porous surface would be no longer useful if the concentration of the reacting species from the bulk solution dropped down to zero at the outer surface layer because of the fast kinetics. Therefore, the advantage of the NPGF electrode could not fully stand out on analyzing redox reactions with fast electron-transfer kinetics.

On the basis of Kuhn's explanation, we expected that a remarkable increase in electrochemical signal at the NPGF electrode could be observed for redox reactions with low electron-transfer kinetics. Therefore, we further applied our NPGF electrode on the oxidation of Fe^{2+} to Fe^{3+} and the reduction of Cu^{2+} to Cu^{+} with slow electron-transfer kinetics. Figure 5c shows the SWV curves conducted in a solution containing 10 mM NH_4FeSO_4. In Figure 5c, the peak at 420 mV originated from the oxidation of Fe^{2+} to Fe^{3+}. As we expected, the anodic SWV current of Fe^{2+} oxidation increased by 2 orders of magnitude at the NPGF electrode. Surprisingly, the signal magnification at the NPGF electrode was extremely high for the Cu^{2+}/Cu^{+} reaction system. In Figure 5d, the reduction wave at 220 mV was caused by the reduction of Cu^{2+} to Cu^{+}. This peak current at the NPGF electrode was found to be about 7000 times higher than that at the polished gold electrode.

3.3. Detection of Dopamine with the Nanoporous Gold Film Electrode. To check the electroanalytical potential of the NPGF electrode obtained after 30 cycles, we applied this electrode to the determination of biomolecule dopamine with low concentration. We found that the NPGF electrode could efficiently accelerate the electrooxidation of dopamine on the Au surface and produce a remarkably larger oxidation current (Figure 6a). The dopamine signal increased by at least 2 orders of magnitude when the NPGF electrode was used instead of the polished gold electrode. The determination of dopamine concentration was performed using square wave voltammetry (SWV) in pH 7.1 phosphate buffer solution (PBS). Figure 6b reveals that the oxidation peak current enhances accordingly with the concentration of dopamine increases from 5 to 30 nM. The calibration plot (inset of Figure 6b) shows a good linear relationship with a correlation coefficient of 0.999 and a slop of 0.38 μA nM^{-1} (95% confidence interval).

It is known that ascorbic acid (AA) and dopamine coexist in the body fluid and that the concentration of AA is much higher than that of dopamine. Therefore, we tested the selectivity of the NPGF electrode toward dopamine under

(24) Szamocki, R.; Velichko, A.; Holzapfel, C.; Mucklich, F.; Ravaine, S.; Garrigue, P.; Sojic, N.; Hempelmann, R.; Kuhn, A. *Anal. Chem.* **2007**, *79*, 533−539.

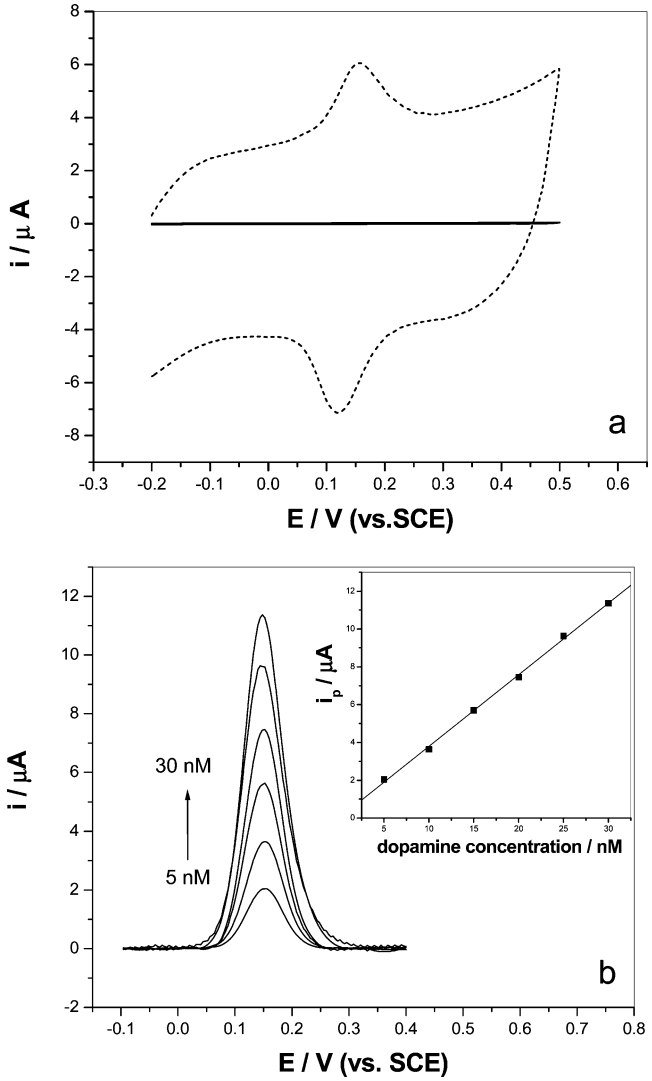

Figure 6. (a) CV curves of 20 nM dopamine in pH 7.1 phosphate buffer solution at the NPGF electrode (dashed line) and the polished gold electrode (solid line), scan rate = 50 mV s^{-1}; (b) SWV curves of 5, 10, 15, 20, 25, and 30 nM dopamine in pH 7.1 phosphate buffer solution at the NPGF electrode with a frequency of 15 Hz, increments of 4 mV, and amplitude of 25 mV. The blank current in SWV was subtracted. The inset of b was the calibration plot of SWV peak current versus concentration of dopamine.

the interference of AA. Figure 7 shows the electrochemical signals of dopamine and AA mixtures at the NPGF electrode. On the SWV curve of a pure 20 μM AA solution, there was a broad peak at about 0.31 V, which corresponded to the oxidation of AA. After adding dopamine into this AA solution, an extra signal corresponding to dopamine oxidation could be easily observed (Figure 7). By subtracting the signal of AA, the electrochemical response of dopamine could be obtained. The plot of peak current against the concentration of dopamine was shown in the inset of Figure 7. The resulting five-point standard curve was of a good linear relationship with a correlation coefficient of 0.995 and a slop of 0.355 μA nM^{-1} (95% confidence interval). The detection limit of dopamine with the NPGF electrode was calculated to be as low as 1 nM.

The NPGF electrode exhibits a better selectivity than the polished electrode for the determination of dopamine in the

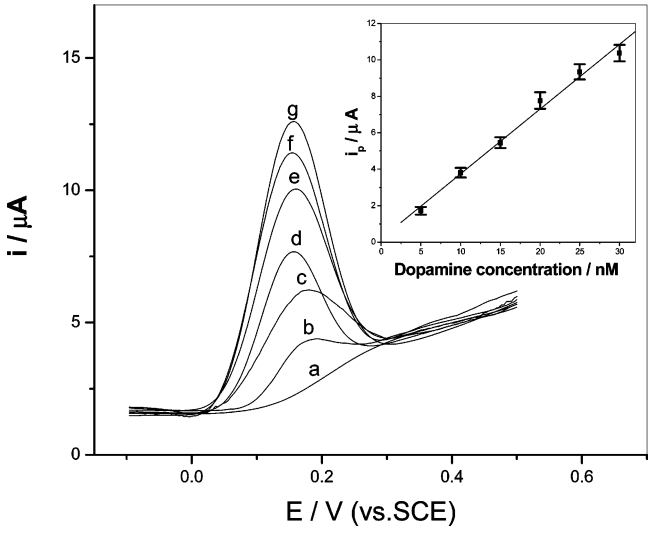

Figure 7. SWV curves of dopamine and ascorbic acid mixtures in pH 7.1 PBS at the NPGF electrode, with a frequency of 15 Hz, increments of 4 mV, and amplitude of 25 mV. The concentration of ascorbic acid was fixed at 20 μM and the dopamine concentrations were (a) 0, (b) 5, (c) 10, (d) 15, (e) 20, (f) 25, and (g) 30 nM. The inset was the calibration plot of SWV peak current versus concentration of dopamine.

presence of ascorbic acid. We attribute the better selectivity to the selective adsorption of dopamine on NPGF electrode. During the electrochemical analysis of dopamine in the presence of ascorbic acid, we surprisingly found that the signal of dopamine could still be detected in blank solution with the used NPGF electrode, even after washing it with deionized water many times. A detailed study on this selective adsorption of dopamine on the NPGF electrode is in progress. Obviously, a NPGF electrode with a high surface area can enhance this selective adsorption, resulting in a correspondingly higher selectivity.

4. Conclusions

In summary, we developed a one-pot green route for fabricating a nanoporous gold film electrode through multicyclic electrochemical alloying/dealloying of a polished gold electrode in a novel electrolyte composed of $ZnCl_2$ and benzyl alcohol. The resulting nanoporous gold film electrode possessed ultrahigh surface area and electrochemical activity as well as good selectivity to dopamine detection. This nanoporous gold film electrode is very promising in many fields, with applications such such as catalysis, sensors, analysis, and so on. Moreover, we believe that this multicyclic electrochemical alloying/dealloying method in benzyl alcohol electrolytes can be applied to prepare other nanoporous metal film electrodes.

Acknowledgment. This work was supported by the National Science Foundation of China (Grants 20503009 and 20673041) and the Open Fund of Key Laboratory of Catalysis and Materials Science of the State Ethnic Affairs Commission & Ministry of Education, Hubei Province (Grants CHCL0508 and CHCL06012).

CM070425L